arXiv:2404.19106v1 [cond-mat.mes-hall] 29 Apr 2024

Bilayer graphene in periodic and quasiperiodic magnetic superlattices

David J. Fernández C.[1,a], O. Pavón-Torres[1,b*]

[1] Physics Department, Cinvestav, POB 14-740, 07000 Mexico City, Mexico

Abstract

Starting from the effective Hamiltonian arising from the tight binding model, we study the behaviour of low-lying excitations for bilayer graphene placed in periodic external magnetic fields by using irreducible second order supersymmetry transformations. The coupled system of equations describing these excitations is reduced to a pair of periodic Schrödinger Hamiltonians intertwined by a second order differential operator. The direct implementation of more general second-order supersymmetry transformations allows to create nonsingular Schrödinger potentials with periodicity defects and bound states embedded in the forbidden bands, which turn out to be associated to quasiperiodic magnetic superlattices.

Keywords— Bilayer graphene, superlattices, second order SUSY QM, Lamé equation.

1 Introduction

The correspondence between band structure of graphene and the topological features of electronic states had played a major role in modern physics since its discovery in 2004 [1]. Due to its honeycomb lattice structure, small local changes lead to gauge potentials, associated with the phase of the electronic wavefunction in each of the two independent sublattices [2]. In particular, the local in-plane deformations generated by strain can be described by a vector potential, which is equivalent to a pseudomagnetic field applied to graphene. The band structure of graphene can be fundamentally changed in different ways, one of which is the stacking of two layers in order to form bilayer graphene [3]. Bilayer graphene presents some advantages over monolayer graphene, since the larger possibilities for tuning experimentally its physical properties [4, 5]. In bilayer graphene there are four atoms per unit cell, with inequivalent sites $A1$, $B1$ and $A2$, $B2$ in the first and second graphene layers, respectively [6]. The atomic orientation among the two layers might further vary, as bilayer graphene has a weak van der Waals interlayer bonding due to lattice deformation, which largely affects the interlayer electron motion [7]. Bilayer graphene can display a parabolic dispersion relation at the K points, making electrons behave differently as compared with the single-layer case. Bilayer graphene offers as well the possibility of applying a bias voltage W between the two layers, allowing to tune the band structure [8]. In particular, the inequivalence of the two graphene layers gives rise to a Mexican-hat-like structure featuring a band gap [3]. Let us stress that a tunable gap is important for possible electronic devices.

Different stackings can occur in bilayer graphene. Due to its large stability in bulk graphite, the most studied is the AB Bernal stacking, in which the two graphene layers are arranged in such a way that the $A1$ sublattice is exactly on top of the $B2$ sublattice. On the other hand, in the simple hexagonal or AA stacking,

*omar.pavon@cinvestav.mx

both sublattices of the first layer, $A1$ and $B1$, are located directly on top of the two sublattices $A2$ and $B2$ of the second layer. Although graphene with direct or AA stacking has not been observed in natural graphite, it has been produced by folding graphite layers at the edges of a cleaved sample with a scanning tunnelling microscope tip. A third simple bilayer structure arises when the two layers are stacked with a specific twisting angle (θ), called twisted bilayer graphene (TBG). In this structure the moiré patterns with a higher periodicity emerge. The emergence of these patterns features remarkable optical and electronic properties [9, 10, 11, 12, 13]. The electronic structure of TBG shows a linear band dispersion near the Dirac points, rather than the massive quadratic dispersion of the AB-stacked bilayer graphene, suggesting a relatively weak interlayer interaction. In strong magnetic fields, however, it is predicted that the spectrum exhibits a fractal structure, called Hofstadter's butterfly, in which a series of energy gaps appear in a self-similar fashion [14].

Due to its Dirac-like low lying excitations, graphene displays a number of unusual transport properties, which results in the pseudospin 1/2 of the low-lying modes, their linear dispersion relation, and the vanishing density of states at the Dirac points. In contrast, the interlayer interaction in bilayer graphene with regular AB stacking changes the linear dispersion of monolayer graphene into a quadratic one, where an electron behaves as a massive particle [15]. In order to describe the situation when magnetic (or pseudomagnetic) fields are applied to monolayer graphene, the first-order supersymmetric quantum mechanics (SUSY QM) is the simplest solution approach [16, 17, 18, 19, 21, 20, 22, 23, 24] (see also [25, 26, 27, 28, 29, 30, 31]). On the other hand, the second-order SUSY QM has proved useful to study the charge carriers behaviour of bilayer graphene in external magnetic fields [32, 33]. In addition, the equivalence between Maxwell's and Dirac equation has been used to understand the electromagnetic spin and orbital angular momentum, and examine the relationship between interface states and topology [34, 35, 36, 37].

Recently, the first order SUSY QM has been used to study the electronic behaviour in *superlattices*, i.e, when monolayer graphene is placed in periodic magnetic fields [38]. The arising of two opposite Darboux displacement breaks the periodicity in the superlattice, but it can be shown that asymptotically the periodicity is recovered. Moreover, the use of such displacements turns out to be fundamental for understanding the phenomenon related to defects in superlattices.

In the present work we aim to study the behaviour of low-lying excitations of bilayer graphene placed in a periodic magnetic field, and its physical implications, by using second order supersymmetric quantum mechanics. We will explore as well more general second-order supersymmetry transformations producing periodicity defects, which will be associated naturally to quasiperiodic magnetic superlatticces for bilayer graphene. In order to do that, the second section is devoted to some general considerations about the tight-binding model for bilayer graphene, its physical assumptions and the two coupled equations we will arrive for our system. Then, in section 3 a brief overview of the second order SUSY QM will be given, as well as the construction of the intertwining operators when a periodic potential is present. The way to implement the method for generating quasiperiodic partner potentials and the corresponding superpotential will be also discussed. In section 4 we will generate the quasiperiodic magnetic superlattices associated to a physically meaningful quantum problem. Finally, in section 5 we will present our conclusions and the perspectives of this work.

2 Tight-binding model for bilayer graphene

As it was already mentioned, among all possible configurations that bilayer graphene may adopt (AA, AB or twisted bilayer), the AB configuration or Bernal stacking is the most stable one, and it is easily produced in labs. In this configuration, half of the carbon atoms of the top layer are aligned vertically with half of the atoms of the lower layer, while the other carbon atoms of the top layer are located above the centres of the lower-layer hexagons. This means that one layer is rotated with respect to the other by an angle of $\pi/3$, and from now on we will address this configuration only.

The effective Hamiltonian around a Dirac point for bilayer graphene is

$$H = \frac{1}{2m^*}\begin{pmatrix} 0 & (p_x - ip_y)^2 \\ (p_x + ip_y)^2 & 0 \end{pmatrix}, \tag{1}$$

where $m^* = \gamma_1/2v_F^2 \approx 0.054m_e$ is the electron effective mass, m_e is the electron free mass, v_F is the Fermi velocity, $p_x = -i\hbar\frac{\partial}{\partial x}$ and $p_y = -i\hbar\frac{\partial}{\partial y}$. We use the minimal coupling rule to incorporate the vector potential, i.e., $p_i \to p_i + \frac{e}{c}A_i$. In the Landau gauge the vector potential can be chosen as $\vec{A} = A(x)\hat{e}_y$, implying that $\vec{B} = B(x)\hat{e}_z$ thus the magnetic field amplitude takes the form $B(x) = A'(x)$. The eigenvalue equation when an external magnetic field is applied is given by:

$$H\Psi(x,y) = \frac{1}{2m^*}\begin{pmatrix} 0 & \Pi^2 \\ (\Pi^+)^2 & 0 \end{pmatrix}\Psi(\mathbf{x}) = E\Psi(\mathbf{x}), \tag{2}$$

with $\Pi = p_x - ip_y - i\frac{e}{c}A(x)$. Taking into account the translation invariance along y direction we propose

$$\Psi(x,y) = e^{iky}\begin{pmatrix} \psi^{(2)}(x) \\ \psi^{(0)}(x) \end{pmatrix}. \tag{3}$$

By sticking to the approach introduced in [32, 33], the following system of equations is obtained:

$$L_2^-\psi^{(0)}(x) = \left(\frac{d^2}{dx^2} + \eta(x)\frac{d}{dx} + \gamma(x)\right)\psi^{(0)}(x) = -\tilde{E}\psi^{(2)}(x), \tag{4}$$

$$L_2^+\psi^{(2)}(x) = \left(\frac{d^2}{dx^2} - \eta(x)\frac{d}{dx} + \gamma(x) - \eta'(x)\right)\psi^{(2)}(x) = -\tilde{E}\psi^{(0)}(x), \tag{5}$$

where $\tilde{E}$ and $\eta(x)$ are given by

$$\tilde{E} = \frac{2m^*E}{\hbar^2}, \qquad \eta(x) = 2\left(k + \frac{e}{c\hbar}A(x)\right). \tag{6}$$

Thus, the magnetic field amplitude $B(x)$ takes the form

$$B(x) = \frac{c\hbar}{2e}\eta'(x). \tag{7}$$

Since we want to study the case when a periodic magnetic field is applied, $\eta(x)$ and $\gamma(x)$ in equations (4) and (5) are supposed to be complex valued piecewise continuous periodic functions, both with the same period. Note that an iterative first order SUSY treatment could be used, such that the second order differential intertwining operators (4) and (5) will be factorized as a product of two in general different first order intertwining operators. These assumptions require to modify the effective Hamiltonian by an additional term, that could be physically interpreted as the result of a trigonal warping effect or a varying external potential. This is expressed mathematically as follows

$$H = \frac{1}{2m^*}\begin{pmatrix} 0 & \Pi^2 \\ (\Pi^+)^2 & 0 \end{pmatrix} - \frac{\hbar^2}{2m^*}f(x)\sigma_x, \tag{8}$$

where

$$f(x) = \frac{\eta'(x)}{4\eta^2(x)} - \frac{\eta''(x)}{2\eta(x)} - \frac{(\epsilon_1 - \epsilon_2)^2}{4\eta^2(x)}. \tag{9}$$

The coupled system of equations (4) and (5) can be decoupled as follows:

$$L_2^+L_2^-\psi^{(0)}(x) = \tilde{E}^2\psi^{(0)}(x), \tag{10}$$

$$L_2^-L_2^+\psi^{(2)}(x) = \tilde{E}^2\psi^{(2)}(x). \tag{11}$$

We have chosen the index notation slightly different from [32, 33], for reasons that will be evident below. As can be seen, in order to study the effect of periodic magnetic fields in bilayer graphene, the second order supersymmetric quantum mechanics can be used, as when studying the charge carriers behaviour of bilayer graphene in non-periodic external magnetic fields. Before doing that, however, a brief overview of the second order supersymmetric quantum mechanics will be given in the following section.

3 Second order supersymmetric quantum mechanics

Let us assume that $v_1(x)$ and $v_2(x)$ are two solutions of the stationary Schrödinger equation for the Hamiltonian H_0 associated to the factorization energies ϵ_1 and ϵ_2, respectively, *i.e.,* $H_0 v_i = \epsilon_i v_i$, $i = 1, 2$, where

$$H_0 = -\frac{d^2}{dx^2} + V_0(x). \tag{12}$$

We will suppose that an intertwining relation involving the two Hamiltonians H_0, H_2 and the operator L_2^- of equation (4) is fulfilled, namely,

$$H_2 L_2^- = L_2^- H_0, \tag{13}$$

where

$$H_2 = -\frac{d^2}{dx^2} + V_2(x). \tag{14}$$

We will assume as well that both Hamiltonians (12) and (14) have discrete spectra. The so-called SUSY partner potentials $V_0(x)$ and $V_2(x)$ can be expressed in terms of the functions $\eta(x)$ and $\gamma(x)$ characterizing the interwining operator L_2^-. After some work, the following expressions are obtained:

$$\gamma(x) = -\frac{\eta^{''}(x)}{2\eta(x)} + \left(\frac{\eta^{'}(x)}{2\eta(x)}\right)^2 + \frac{\eta^{'}(x)}{2} + \frac{\eta^2(x)}{4} - \left(\frac{\epsilon_1 - \epsilon_2}{2\eta(x)}\right)^2, \tag{15}$$

where $\eta(x)$ is given by

$$\eta(x) = -\frac{d}{dx} \ln W(v_1(x), v_2(x)) = \frac{(\epsilon_1 - \epsilon_2) v_1(x) v_2(x)}{W(v_1(x), v_2(x))}, \tag{16}$$

with $W(v_1(x), v_2(x)) \equiv W_{12}(x)$ being the Wronskian of $v_1(x)$ and $v_2(x)$. The partner potentials $V_0(x)$ and $V_2(x)$ turn out to be expressed as:

$$V_0(x) = \frac{\eta^{''}(x)}{2\eta(x)} - \left(\frac{\eta^{'}(x)}{2\eta(x)}\right)^2 - \eta^{'}(x) + \frac{\eta^2(x)}{4} + \left(\frac{\epsilon_1 - \epsilon_2}{2\eta(x)}\right)^2 + \frac{\epsilon_1 + \epsilon_2}{2}, \tag{17}$$

$$V_2(x) = \frac{\eta^{''}(x)}{2\eta(x)} - \left(\frac{\eta^{'}(x)}{2\eta(x)}\right)^2 + \eta^{'}(x) + \frac{\eta^2(x)}{4} + \left(\frac{\epsilon_1 - \epsilon_2}{2\eta(x)}\right)^2 + \frac{\epsilon_1 + \epsilon_2}{2}. \tag{18}$$

Notice that the new potential $V_2(x)$ can be simply expressed as:

$$V_2(x) = V_0(x) + 2\eta^{'}(x) = V_0(x) - 2\frac{d^2}{dx^2}\left(\ln W_{12}(x)\right). \tag{19}$$

It will be free of singularities whenever $W_{12}(x)$ is nodeless. The eigenfunctions of H_0 and H_2, $\{\psi_i^{(0)}(x), \psi_i^{(2)}(x), i = 0, 1, \dots\}$, are connected by the operators L_2^-, L_2^+ as follows:

$$L_2^- \psi_i^{(0)} = \frac{W(v_1, v_2, \psi_i^{(0)}(x))}{W_{12}(x)} \propto \psi_i^{(2)}(x). \tag{20}$$

From equation (20) it is clear that $L_2^- v_1(x) = L_2^- v_2(x) = 0$. Moreover, the kernel of L_2^+ supplies two formal eigenfunctions of H_2 associated to ϵ_1 and ϵ_2:

$$v_1^{(2)}(x) \propto \frac{v_2(x)}{W_{12}(x)}, \quad v_2^{(2)}(x) \propto \frac{v_1(x)}{W_{12}(x)}. \tag{21}$$

Depending on whether they can be normalized or not, such factorization energies can be either included or not in the spectrum of H_2. Therefore, the Hamiltonians H_0 and H_2 are isospectral, with the possible exception of ϵ_1 and ϵ_2, which could be in $\mathrm{Sp}(H_2)$. From now on we will assume that $V_0(x)$ is a given initial periodic potential of period T, $V_0(x+T) = V_0(x)$. In this case there is no need to consider the range of the variable x as the whole real line, but just a given period. According to the Bloch-Floquet theory, the physical wavefunctions $\psi(x)$ are quasi-periodic:

$$\psi(x+T) = e^{ikT}\psi(x), \tag{22}$$

where $k \in \mathbb{R}$ is called quasi-momentum or momentum of the crystal, and it defines a self-adjoint boundary value problem.

3.1 Lamé equation: some remarks

In order to study the effect of periodic potentials on bilayer graphene we start with the Lamé potential

$$V_0(x) = n(n+1)m\,\mathrm{sn}^2(x|m). \tag{23}$$

The stationary Schrödinger equation for the Hamiltonian (12) with the periodic potential given by expression (23) is the Jacobi version of the *Lamé equation*, where $\mathrm{sn}(x|m)$ is the Jacobi elliptic function in Glaisher notation with modular parameter m. When $m \in (0,1)$ the function $\mathrm{sn}^2(x|m)$ has real period $2K = 2K(m)$ and an imaginary period $2iK' = 2iK(1-m)$, with $K(m)$ being the first complete elliptic integral. In addition, if x is restricted to the real axis and m and n are real, the Lamé equation becomes a real domain Schrödinger equation with a periodic potential, i.e., a Hill's equation.

The potential (23) has bounded physical solutions (22) with an energy spectrum consisting of exactly $n+1$ allowed bands separated to each other by $n+1$ forbidden bands [39, 40]. The band edges arise when $kT = 0, \pi, ...$, i.e., for

$$\psi(x+T) = e^{ikT}\psi(x) = \xi\psi(x), \tag{24}$$

with $\xi = \pm 1$ being a Floquet multiplier. Due to the fact that the H_0 in Eq. (12) with the $V_0(x)$ given by expression (23) is a Lamé operator of Hill type, we know from the oscillation theorem that there exists a sequence of real numbers (in general infinite)

$$E_0 < E_1 \leq E_{1'} < E_2 \leq \cdots < E_j \leq E_{j'} < \ldots, \quad j = 1, 2, ... \tag{25}$$

where the band edge energies E_j and $E_{j'}$ correspond to $2K$-periodic solutions for j even and $2K$-antiperiodic solutions for j odd. The physical energies lie in allowed bands, which are intervals delimited by energies corresponding to the two values of ξ, i.e., to periodic and anti-periodic Bloch solutions. These allowed bands form a sequence, where E_0 is the first periodic eigenvalue if we come from $-\infty$, followed by alternating pairs of anti-periodic and periodic eigenvalues (each pair may be coincident). The allowed energy bands are $[E_0, E_1]$, $[E_{1'}, E_2], ..., [E_{j'}, E_{j+1}], ...$; consistently, the forbidden energy bands (energy gaps) are $(E_1, E_{1'})$, $(E_2, E_{2'}), ..., (E_j, E_{j'}), ...$ The band edge energies are usually called the discrete spectrum of the periodic potential. The corresponding eigenfunctions $\{\psi_0^{(0)}, \psi_1^{(0)}, \psi_{1'}^{(0)}, \psi_2^{(0)}, \psi_{2'}^{(0)}, \ldots\}$ have periods T, $2T$, $2T$, T, T, $\ldots$, and their respective number of nodes in a period T is $0, 1, 1, 2, 2, \ldots$.

Many algebraic forms can be obtained from expression (23); nevertheless, for studying the properties of the Lamé equation it is important to take a form appropriate for the purposes at hand. For practical applications the Jacobian form, leading to the theta-functions, is the most suitable one. On the other

hand, for studying the properties of the solutions it is better to use the second algebraic form, although in some problems the analysis is simpler using the Weierstrass form [50]. Let us stress that the Jacobi elliptic and Weierstrass functions have been widely used in the description of physical phenomena [41, 42, 43, 44]. Recently, this interest has been renewed since they have been employed in direct methods for solving nonlinear differential equations [45, 46, 47, 48].

Let us express the Lamé equation in terms of the Weierstrass function $\wp = \wp(u; g_2, g_3)$, which is a canonical elliptic function with a double pole at $u = 0$ satisfying

$$(\wp')^2 = 4(\wp - e_1)(\wp - e_2)(\wp - e_3). \tag{26}$$

For ellipticity, the roots $\{e_\gamma\}_{\gamma=1}^3$ must be different, which is equivalent to ask that the modular discriminant $\Delta = g_2^3 - 27g_3^2$ should be non-zero. Either of $g_2, g_3 \in \mathbb{C}$ may be equal to zero, but not both of them. The relation between the Jacobi and Weierstrass elliptic functions is well known. Choose, first $\{e_\gamma\}_{\gamma=1}^3$ in the way:

$$(e_1, e_2, e_3) = A^2 \left(\frac{2-m}{3}, \frac{2m-1}{3}, -\frac{m+1}{3} \right), \tag{27}$$

where $A \in \mathbb{C}/\{0\}$ is any proportionality constant. Then,

$$g_2 = A^4 \frac{4(m^2 - m + 1)}{3}, \qquad g_3 = A^6 \frac{4(m-2)(2m-1)(m+1)}{27}, \tag{28}$$

and the dimensionless (A-independent) Klein invariant $J = g_2^3/\Delta$ is given by

$$J = \frac{4}{27} \frac{(m^2 - m + 1)^3}{m^2(1-m)^2}. \tag{29}$$

Two sorts of elliptic function are related with $\wp$ as follows:

$$\mathrm{sn}^2(Az|m) = \frac{e_1 - e_2}{\wp(z) - e_3}, \qquad \mathrm{ns}^2(Az|m) = \frac{\wp(z) - e_3}{e_1 - e_3}, \tag{30}$$

thus the periods of $\wp$, denoted 2ω, $2\omega'$, will be related to those of sn^2 by

$$2\omega = \frac{2K}{A}, \qquad 2\omega' = \frac{2iK'}{A}. \tag{31}$$

The case when $2K$, $2K'$ are real, or equivalently $\omega \in \mathbb{R}$, $\omega' \in i\mathbb{R}$, corresponds to the case when $g_2, g_3 \in \mathbb{R}$ and $\Delta > 0$. Choosing now for simplicity $A = 1$, so that $e_1 - e_3 = A^2 = 1$, we can rewrite the Lamé equation with the aid of (30) in its Weierstrass form:

$$\left\{ \frac{d^2}{du^2} - [n(n+1)\wp(u; g_2, g_3) + B] \right\} \psi = 0, \tag{32}$$

where $u = x + iK'$. Note that the translation of (23) by iK' replaces $m\,sn^2$ by ns^2. Moreover, $B = -E(e_1 - e_3) - n(n+1)e_3$, *i.e.*,

$$B = -E + \frac{1}{3} n(n+1)(m+1), \tag{33}$$

is a transformed energy parameter.

Because for $n = 1$ the hyperbolic limit yields a bound state at $E = 0$, and scattering states above $E = 1$, for the periodic case we would expect to see at least an energy band with one edge at $E = 0$. Therefore, another band edge energies ought to be below $E = 1$. The band edge eigenstates found explicitly are $\mathrm{dn}(x, m)$, $\mathrm{cn}(x, m)$ and $\mathrm{sn}(x, m)$, with an allowed band energy going from $E = 0$ to $E = 1 - m$, then a band gap, and finally an infinite band energy starting from $E = 1$. In order to find the remaining states, a formal solution of the eigenvalue problem for the Hamiltonian H_0 is necessary. This problem can be expressed as

$$\psi''(x) = (2m\,\mathrm{sn}(x, m)^2 - m - E)\psi(x), \tag{34}$$

or, alternatively,

$$\frac{d^2\psi}{du^2} - [2\wp(u; g_2, g_3) + B]\psi = 0, \tag{35}$$

which is a special case of the Lamé differential equation, whose solution is shown in [49, 50, 51]. In the considered case ($n = 1$) the solution is given by the following independent functions

$$\psi(x, k) = \frac{\sigma(x + k)}{\sigma(x)\sigma(k)} \exp(-\zeta(k)x), \tag{36}$$

where $k \in \mathbb{C}$ and $\sigma(x)$ and $\zeta(x)$ are the Weierstrass σ and ζ functions. Such solutions have the Floquet property

$$\psi(x + 2\omega, k) = \exp(2\eta k - 2\sigma(k)\omega)\psi(x, k), \tag{37}$$

with $\eta = \zeta(\omega)$. In terms of Jacobi elliptic functions the potential (23) for $n = 1$ shifted by the energy $-m$, has the following band edge eigenvalues and eigenfunctions:

$$E_0 = 0, \qquad \psi_0^{(0)}(x) = \mathrm{dn}(x), \tag{38}$$

$$E_1 = 1 - m, \qquad \psi_1^{(0)}(x) = \mathrm{cn}(x), \tag{39}$$

$$E_{1'} = 1, \qquad \psi_{1'}^{(0)}(x) = \mathrm{sn}(x). \tag{40}$$

4 Bilayer graphene in periodic magnetic fields

For a periodic potential $V_0(x)$ every finite energy gap is limited by two eigenfunctions $\psi_j^{(0)}(x)$ and $\psi_{j'}^{(0)}(x)$, $j = 1, 2, ...$, which have the same number of nodes (j). This suggests to take both eigenfunctions to implement a second-order SUSY transformation because we will obtain a physically acceptable partner Hamiltonian H_2 with a non-singular, periodic potential $V_2(x)$. Due to the periodicity T of the intertwining operator L_2^- any eigenfunction $\psi_i^{(0)}$ of the discrete spectrum of H_0 will be transformed by the action of L_2^- into an eigenfunction $\psi_i^{(2)}(x)$ of the discrete spectrum of H_2. Thus, H_0 and H_2 are isospectral Hamiltonians sharing the same band structure [60].

If we replace now the band edge solutions $\psi_1^{(0)}$ and $\psi_{1'}^{(0)}$ in equations (16-18) it turns out that the two SUSY partner potentials differ just by a displacement in the argument i.e., $V_2(x) = V_0(x + K(m))$. The form of the potentials is formally different, but in fact there is no any new physical information due to

$$V_0(x) = 2m\,\mathrm{sn}^2(x, k) - m, \tag{41}$$

$$V_2(x) = 2m\,\mathrm{sn}^2(x + K(m), k) - m. \tag{42}$$

This happens since it is known that the self-isospectrality condition is fulfilled if $\psi_j^{(0)}(x)\psi_j^{(0)}(x + T/2) \propto \psi_{j'}^{(0)}(x)\psi_{j'}^{(0)}(x + T/2)$ [60, 61]. In our case, choosing the band edge eigenfunctions $\psi_1^{(0)}$ and $\psi_{1'}^{(0)}$ given in equations (39) and (40) we will have

$$\mathrm{cn}(x, m)\mathrm{cn}(x + T/2, m) \propto \mathrm{sn}(x, m)\mathrm{sn}(x + T/2, m), \tag{43}$$

which is the condition for $V_2(x)$ to be physically equivalent (self-isospectral) to $V_0(x)$. Thus, there is no new potential obtained for $n = 1$ if band edge eigenfunctions are used. However, for the Lamé potential (23) with $n = 2, 3, ...$, the self-isospectrality condition is not longer fulfilled, and thus new potentials could be obtained [52, 53, 54].

Let us point out that the general Darboux-Crum transformations have been applied to the single gap periodic Lamé potential to generate an arbitrary countable set of bound states in its two forbidden bands,

the infinite lowest and the finite intermediate one. As a consequence, nonperiodic single gap potentials arise, which contain two essentially different types of soliton deffects in the periodic background [56, 57]. As it was already shown, these defects appear in a natural way in carbon-based crystals such as monolayer graphene [38] and, as we will see below, for bilayer graphene. In order to do that, we need to use as seed solutions linear combinations of the two generalized Bloch functions belonging to the same spectral gap in order to obtain the new potential. In this way, the second-order transformation will produce a quasi-periodic magnetic superlattice supporting two bound states.

Let us start from the Lamé magnetic superlattice; the seed solutions we will consider are $v_j = u_1(x,\epsilon_j) + \eta_j u_2(x,\epsilon_j)$, $j = 1, 2$ with $\epsilon_2 < \epsilon_1 < 0$, which fulfill the Lamé equation. The two Bloch functions u_j take the form

$$u_1(x,\epsilon_j)=\frac{\sigma(x_0+\omega')\sigma(x+\delta_j+\omega')}{\sigma(x+\omega')\sigma(x_0+\delta_j+\omega')}e^{-\zeta(\delta_j)(x-x_0)},\ u_2(x,\epsilon_j)=\frac{\sigma(x_0+\omega')\sigma(x-\delta_j+\omega')}{\sigma(x+\omega')\sigma(x_0-\delta_j+\omega')}e^{\zeta(\delta_j)(x-x_0)}, \tag{44}$$

where $j = 1, 2$, x_0 is a fixed point in $[0, T = 2K]$, $\omega = K$ and $\omega = iK'$ are the real and imaginary half-periods of the Jacobi elliptic functions, σ and ζ are the nonelliptic Weierstrass functions, while the factorization energy ϵ_j and the displacement δ_j are related by

$$\epsilon_j = \frac{2}{3}(m+1) - \wp(\delta_j) - m. \tag{45}$$

A short hand notation for $u(x,\epsilon_j)$ in the Wronskians will be employed

$$W(v_1,v_2) = W(\delta_1,\delta_2) + \eta_1 W(-\delta_1,\delta_2) - \eta_2 W(\delta_1,-\delta_2) - \eta_1\eta_2 W(-\delta_1,-\delta_2), \tag{46}$$

with

$$W(\delta_1,\delta_2) = \frac{\sigma^2(x_0+\omega')\sigma(\delta_2-\delta_1)}{\sigma(\delta_1)\sigma(\delta_2)\sigma(x_0+\delta_1+\omega')\sigma(x_0+\delta_2+\omega')}\frac{\sigma(x+\delta_1+\delta_2+\omega')}{\sigma(x+\omega')}e^{-[\zeta(\delta_1)+\zeta(\delta_2)](x-x_0)}, \tag{47}$$

where we have used the symmetry of the quasi-periodic elliptic sigma and zeta functions $\sigma(-x;g_2,g_3) = -\sigma(x;g_2,g_3)$ and $\zeta(-x;g_2,g_3) = -\zeta(x;g_2,g_3)$, respectively. In order to obtain the explicit expression for the magnetic field generated by supersymmetry we replace the expressions (46-47) in (16).

In particular, for the limit case $\eta_1 \to 0$ and $\eta_2 \to 0$ the Wronskian (46) becomes (47), which is consistent with [61]. In the general case, the explicit expression for the magnetic field with impurities is obtained by replacing Eq. (44) in (7):

$$\begin{aligned} B(x;\epsilon_1,\epsilon_2) \propto\ & dn^2(x|m) - dn^2(x+\delta_1+\delta_2|m) + \eta_1\eta_2(dn^2(x-\delta_1-\delta_2|m) - dn^2(x|m)) \\ & + \eta_1(dn^2(x|m) - dn^2(x-\delta_1+\delta_2|m)) + \eta_2(dn^2(x|m) - dn^2(x+\delta_1-\delta_2|m)), \end{aligned} \tag{48}$$

with asymptotic behaviour given by ($x \to \pm\infty$)

$$B(x\to\infty;\epsilon_1,\epsilon_2) \to \eta_1\eta_2(dn^2(x-\delta_1-\delta_2|m) - dn^2(x|m)), \tag{49}$$

$$B(x\to-\infty;\epsilon_1,\epsilon_2) \to dn^2(x|m) - dn^2(x+\delta_1+\delta_2|m). \tag{50}$$

As it was expected, the expressions for the magnetic field with two added impurities are similar to the ones obtained for the case of a single displacement with an added impurity [38]. It is straightforward to find the expressions for the added bound states in the forbidden band $(E_1, E_{1'})$ for bilayer graphene, which arise from equation (21) using linear combinations v_1 and v_2 of the Bloch functions (see a plot in Fig. 1a). Let us stress that, the implementation of the second order supersymmetry transformation for bilayer graphene is mandatory, unlike what happens for monolayer graphene in which an additional SUSY transformation could be applied to go deeper in the study of impurity effects, but it is not strictly required.

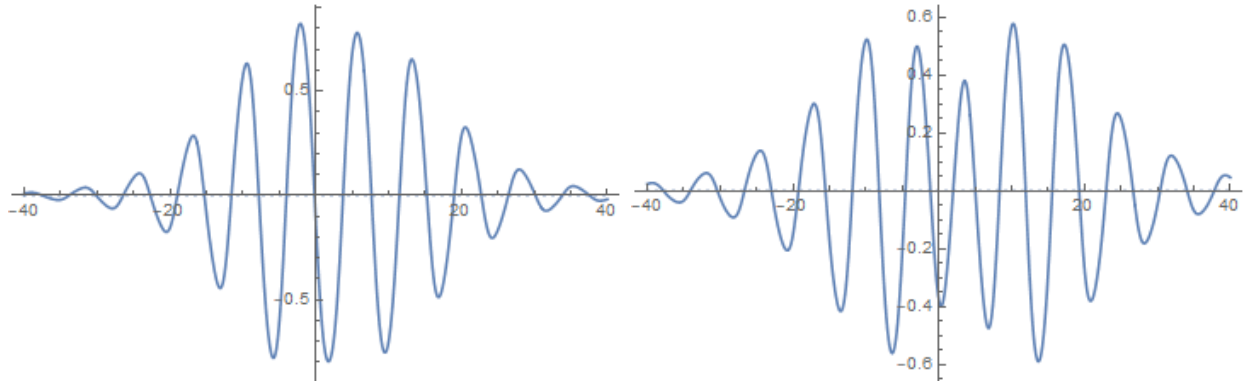

(a) (b)

Figure 1: (a) Bound states created at the energy $\alpha_1 = 0.9$ and at $\alpha_2 = 0.8$ (b) for $m = 0.5$.

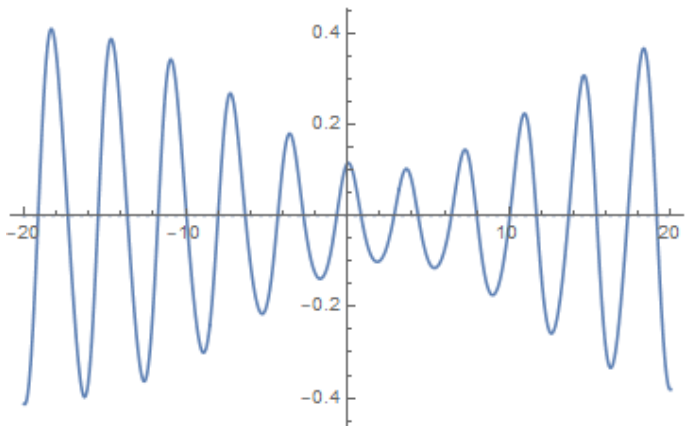

Figure 2: Quasiperiodic magnetic superlattice generated by applying a second order SUSY transformation to bilayer graphene.

The magnetic field amplitude (48) is depicted in Figure 2. From such explicit expression, and the corresponding asymptotic behaviours (49) and (50) for $x \pm \infty$, we can see that the magnetic field recovers its periodicity asymptotically. Throughout this work we have restricted ourselves to study the effect of the Lamé periodic potentials in bilayer graphene; nevertheless, the basic ideas of this work could be applied to more general potentials, e.g., to the associated Lamé potentials [54, 58, 59]. We are confident that the basic idea of introducing defects in the periodic magnetic superlattice for bilayer graphene by adding bound states in the forbidden bands, can be well understood through one of the simplest periodic potentials at hand.

5 Conclusions

Starting from the tight binding model for the low-lying excitations of bilayer graphene, we have determined the energy band structure of bilayer graphene when a periodic magnetic field is applied. In this approach, which generalizes previous works about monolayer graphene, we have employed second order SUSY transformations to deal with the topological features of electronic states in bilayer graphene. The bound states created by the transformations are often related to impurities or van Hove singularities. Alike to the case of monolayer graphene, the implementation of the most general Darboux transformation breaks the periodicity of the originally periodic magnetic field, due to the introduction of such bound states. However, afar from these introduced defects in graphene the solutions turn out to be periodic, behaving as it was expected. It is worth to note that the number of experimental studies about electronic transitions have increased in the

last years, with its optimization being a major concern. About this point, the present study mimics the effect of gold island-enhanced multiplex quantum dots, in which the quantum dots act as a bridge between the gold islands. On the other hand, the present analysis reinforces the role of the second order supersymmetric quantum mechanics for studying electronic properties of bilayer graphene. Throughout this work we restricted ourselves to the simplest case of the Lamé potentials; nevertheless, we might choose, between a long list of candidates, another examples to illustrate the effects of the Darboux transformations for bilayer graphene.

Acknowledgments

The authors acknowledge the support of Consejo Nacional de Humanidades Ciencia y Tecnología (CONAHCyT-México) under grant FORDECYT-PRONACES/61533/2020. OPT acknowledges CONAHCyT by a postdoctoral fellowship.

Data Availability Statement Data sharing not applicable to this article as no datasets were generated or analyzed during the current study.

References

[1] K. S. Novoselov, A. K. Geim, S. V. Morozov, D. Jiang, Y. Zhang, S. V. Dubonos, I. V. Grigorieva and A. A. Firsov. Electric field effect in atomically thin carbon films. Science 306 (5696).

[2] J. W. González, H. Santos, M. Pacheco, L. Chico and L. Brey. Electronic transport through bilayer graphene flakes. Phys. Rev. B 81 (2010).

[3] B. Verbeck, B. Partoens, F. M. Peeters and B. Trauzettel. Strain-induced band gaps in bilayer graphene. Phys. Rev. 85 (2012).

[4] Amol Nimbalkar and Hyunmin Kim. Opportunities and Challenges in Twisted Bilayer Graphene. Nano-Micro Lett. 12:126 (2020).

[5] Pilkyung Moon and Mikito Koshino. Energy spectrum and quantum Hall effect in twisted bilayer graphene. Physical Review B 85 (2012).

[6] Katsnelson, M. The Physics of Graphene (2nd ed.). Cambridge University Press (2020).

[7] Gao Yang, Lihua Li, Wing Bun Lee and Man Cheung Ng. Structure of graphene and its disorders: a review. Science and technology of advanced materials. Sci. Technol. Adv. Mater. 19:1 (2018).

[8] Rui-Ning Wang, Guo-Yi Dong, Shu-Fang Wang, Guang-Sheng Fu and Jiang-Long Wang. Intra- and inter-layer charge redistribution in biased bilayer graphene. AIP Advances 6: 3 (2016).

[9] Jie Wang, Yunqin Zheng, Andrew J. Millis and Jennifer Cano. Chiral approximation to twisted bilayer graphene: Exact intravalley inversion symmetry, nodal structure, and implications for higher magic angles. Physical Review Research **3** (2021).

[10] Haoning Tang, Fan Du, Stephen Carr, Clayton DeVault, Olivia Mello and Eric Mazur. Modeling the optical properties of twisted bilayer photonic crystals. Light Sci. Appl. 10, 157 (2021).

[11] Gustav Chaudhary, A. H. MacDonald and M. R. Norman. Quantum Hall superconductivity from moiré Landau levels. Physical Review Research 3 (2021).

[12] Stephen Carr, Daniel Massatt, Shiang Fang, Paul Cazeaux, Mitchell Luskin and Efthimios Kaxiras. Twistronics: Manipulating the electronic properties of two-dimensional layered structures through their twist angle. Physical Review B 95 (2017).

[13] Muzzamal Iqbal Shaukat, Montasir Qasymeh and Hichem Eleuch. Spatial solitons in an electrically driven graphene multilayer medium. Scientific Reports 12, 10931 (2022).

[14] Yasuyuki Hatsuda, Hosho Katsura and Yuji Tachikawa. Hofstadter's butterfly in quantum geometry. New J. Phys. 18, 103023 (2016).

[15] A. K. Geim. Graphene: Status and Prospects. Science 324, 5934 (2009).

[16] Kuru S., Negro J. and Nieto, L. M. Exact analytic solutions for a Dirac electron moving in graphene under magnetic fields. J. Phys.: Condens. Matter 21, 455305 (2009).

[17] Enrique Milpas, Manuel Torres and Gabriela Murguía. Magnetic field barriers in graphene: analytically solvable model. J. Phys.: Condens. Matter 23, 245304 (2011).

[18] B. Midya and D.J. Fernández C. Dirac elecron in graphene under supersymmetry generated magnetic fields. J. Phys. A: Math. Theor. **47**, 285302 (2014) .

[19] M. Castillo-Celeita and David J. Fernández C. Dirac elecron in graphene with magnetic fields arising from first-order interwining operators. J. Phys. A: Math. Theor. 53, 035302 (2020).

[20] M. Castillo-Celeita, Alonso Contreras-Astorga and David J. Fernández C. Complex supersymmetry in graphene. Eur. Phys. J. Plus 137, 904 (2022).

[21] D. J. Fernández C. and Juan D. García-Muñoz. Graphene in complex magnetic fields. Eur. Phys. J. Plus 137, 1013 (2022).

[22] Dai-Nam Le, Van-Hoang Le, Pinaki Roy. Generalized harmonic confinement of massless Dirac fermions in (2+1) dimensions. Physica E 102 (2018).

[23] Y. Concha-Sánchez, E. Díaz- Bautista and A. Raya. Ritus functions for graphene-like systems with magnetic fields generated by first-order intertwining operators. Phys. Scri. 97, 095203 (2022).

[24] M. Castillo-Celeita, V. Jakubský and K. Zelaya. Form-preserving Darboux transformations for 4×4 Dirac equations. Eur. Phys. J. Plus 137, 3 (2022).

[25] A. Schulze-Halberg and P. Roy. Construction of zero-energy states in graphene through the supersymmetry formalism. J. Phys. A: Math. Theor. 50, 365205 (2017).

[26] A. Schulze-Halberg and P. Roy. Dirac systems with magnetic field and position-dependent mass: Darboux transformations and equivalence with generalized Dirac oscillators. Ann. Phys. 431, 168534 (2021).

[27] M. V. Ioffe and D. N. Nishnianidze. A new class of solvable two-dimensional scalar potentials for graphene. Eur. Phys. J. Plus 137, 1195 (2022).

[28] M. V. Ioffe and D. N. Nishnianidze. Solvable two-dimensional Dirac equation with matrix potential: graphene in external electromagnetic field. symmetry 16, 126 (2024) .

[29] G. Junker. Supersymmetric Dirac Hamiltonian in (1+1) dimensions revisited. Eur. Phys. J. Plus 135, 464 (2020).

[30] B. Bagchi and R. Ghosh. Dirac Hamiltonian in a supersymmetric framework. J. Math. Phys. 62, 072101 (2021).

[31] B. Bagchi, A. Gallerati and R. Ghosh. Dirac equation in curved spacetime: the role of local Fermi velocity. Eur. Phys. J. Plus 138, 1037 (2023).

[32] David J. Fernández, Juan D. García M., Daniel O-Campa. Electron in bilayer graphene with magnetic fields leading to shape invariant potentials. J. Phys. A: Math. Theor. 53, 435202 (2020).

[33] David J. Fernández, Juan D. García M., Daniel O-Campa. Bilayer graphene in magnetic fields generated by supersymmetry. *J. Phys. A: Math. Theor.* **54**, 245302 (2021).

[34] Nitish Chandra & Natalia M. Litchinitser. Photonic bandgap engineering using second-order supersymmetry. Commun. Phys. 4, 59 (2021).

[35] Carlos García-Meca, Andrés Macho Ortiz and Robert Llorente Sáez. Supersymmetry in the time domain and its application in optics. Nat. Commun. 11, 813 (2020).

[36] Michael Tomka, Mikhail Pletyukhov and Vladimir Gritsev. Supersymmetry in quantum optics and in spin-orbit coupled systems. Sci. Rep. **5**, 13097 (2015).

[37] Galaktionov, Artem V. Supersymmetric Hamiltonian solutions simulated by Andreev bound states. Physical Review B 101, 134501 (2020).

[38] Miguel Castillo-Celeita, Alonso Contreras-Astorga and David J. Fernández C. Design of quasiperiodic magnetic superlattices and domain walls supporting bound states. Eur. Phys. J. Plus 138, 820 (2023).

[39] William A. Haese-Hill, Martin A. Hallnäs and Alexander P. Veselov. On the spectra of real and complex Lamé operators. SIGMA **13**, 049 (2017).

[40] Robert S. Maier. Lamé polynomials, hyperelliptic reductions and Lamé band structure. Phil. Trans. R. Soc. A **366** (2008).

[41] William A. Schwalm. (2015). Lectures on Selected Topics in Mathematical Physics: Elliptic Functions and Elliptic Integrals. Morgan & Claypool Publishers.

[42] Georgios Pastras (2020). The Weierstrass Elliptic Fuction and Applications in Classical and Quantum Mechanics. Springer.

[43] M. P. Grosset & A.P. Veselov. Lamé equation, quantum Euler top and elliptic Bernoulli polynomials. Proceedings of the Edinburgh Mathematical Society 51 (2008).

[44] Alain J. Brizard. A primer on elliptic functions with applications in classical mechanics. Eur. J. Phys. **30**, 729 (2009) .

[45] Yong Chen, Zhenya Yan. The Weierstrass elliptic function expansion method and its applications in nonlinear wave equations. Chaos, Solitons and Fractals 29, 4 (2006).

[46] Ahmad T. Ali. New generalized Jacobi elliptic function rational expansion method. Journal of computational and applied mathematics 235, 14 (2011).

[47] Abdelfattah El Achab. Constructing of exact solutions to the nonlinear Schrödinger equation (NLSE) with power-law nonlinearity by the Weierstrass elliptic function method. Optik 127, 3 (2016).

[48] Tatyana Belyaeva Leonidovna, Máximo Augusto. Agüero Granados, Omar Pavón Torres (2023). Retos de física nuclear y fenónemos no lineales (1 ed.) Ciudad de México: McGraw-Hill/UAEMéx.

[49] A. Erdely. Trascendental Functions, vol. 2 (McGraw- Hill Company Inc, New York, 1953), p. 1953.

[50] E. Whittaker, G. Watson, A course of Modern Analysis, Cambridge Mathematical Library (Cambridge University Press, Cambridge, 1950).

[51] F. M. Arscott, Periodic Differential Equations: An introduction to Mathieu, Lamé and Allied Functions (Pergamon Press, Oxford, 1964).

[52] Gerard Dunne and Joshua Feinberg. Self-isospectral periodic potentials and supersymmetric quantum mechanics. Phys. Rev. D 57, 1271 (1998).

[53] Tomoaki Nagasawa, Satoshi Ohya, Kazuki Sakamoto, Makoto Sakamoto and Kosuke Sekiya. Hierarchy of QM SUSYs on a bounded domain. J. Phys. A: Math. Theor. 42, 265203 (2009).

[54] Avinash Khare & Uday Sukhatme. Periodic potentials and supersymmetry. J.Phys. A: Math. Gen. 37, 10037 (2004).

[55] Gerald V. Dunne & M. Shifman. Duality and self-duality (energy reflection symmetry) of quasi-exactly solvable periodic potentials. Annals of Physics 299, 2 (2002).

[56] David J. Fernández C., Bodgan Mielnik and Oscar Rosas-Ortiz. Nonlocal supersymmetric deformations of periodic potentials. J. Phys. A: Math. Gen. 35 (2002).

[57] Adrián Arancibia, Francisco Correa, Vit Jakubský, Juan Mateos Guilarte and Mikhail S. Plyuschchay. Soliton defects in one-gap periodic system and exotic supersymmetry. Physical Review D 90, 125041 (2014).

[58] David J. Fernández and Aish Ganguly. Exactly solvable associated Lamé potentials and supersymmetric transformations. Annals of Physics 322, 5 (2007).

[59] David J. Fernández and Asish Ganguly. New supersymmetric partners for the associated Lamé potentials. Physics Letters A 338, 3-5 (2005).

[60] David J. Fernández C., Javier Negro and Luis M. Nieto. Second-order supersymmetric periodic potentials. Physics Letters A 275, 5-6 (2000).

[61] David J. Fernández, Bodgan Mielnik, Oscar Rosas-Ortiz and Boris F. Samsonov. The phenomenon of Darboux displacements. Physics Letters A 294, 3-4 (2002).